Frontiers in Computing and Intelligent Systems
ISSN: 2832-6024 | Vol. 11, No. 3, 2025

Research on Intelligent Anti-Jamming for Data Links Based on CV-R-BiLSTM-A Interference Recognition Network

Xiaoyu Zhang, Xiang Ji, Yize Li

Xijing University, Xi'an, Shaanxi, China

Abstract: The interference recognition module, as a key part of intelligent anti-jamming models, is the cornerstone of intelligent anti-jamming technology. In data link communications, if interference can be effectively detected and the type of interference signal identified, effective anti-jamming measures can be implemented to mitigate the impact of interference on communication quality. Given the current lack of interference signal recognition methods and the low overall recognition rate of existing methods, this paper proposes an interference recognition network method based on complex-valued residual bidirectional long short-term memory attention (CV-R-BiLSTM-A) to identify interference signals. This network improves the overall recognition rate by about 10%. When the signal-to-noise ratio (SNR) is greater than 5 dB, the recognition ability of the CV-R-BiLSTM-A network is more advantageous, with a recognition rate of over 95%, while other networks have recognition rates between 80% and 90%.

Keywords: CV-R-BiLSTM-A Interference Recognition Network; Intelligent Anti-Jamming for Data Links; Interference Recognition Module.

1. Introduction

With the development of information technology, informatization and networking dominate modern warfare. Mastering the initiative of information means controlling the victory of the war. Link 16 enhances the combat capability by sharing information and helps the United States win in the wars in Afghanistan and Iraq, highlighting the importance of data links in information warfare. In electronic countermeasure warfare, it is necessary to ensure the operation of one's own data link and destroy the enemy system. Anti-jamming technology has become a research hotspot. Interference is divided into natural and man-made (with the focus on intentional interference). This paper focuses on barrage jamming in suppressive jamming. Anti-jamming technologies are divided into spread spectrum (such as DSSS, FHSS, etc., adopted by Link 16) and non-spread spectrum technologies (such as adaptive filtering, smart antennas). Currently, non-spread spectrum technologies, especially intelligent anti-jamming technologies, are receiving attention, including interference identification, decision-making, and suppression. Using deep learning to improve the feature extraction ability is of great significance to the future development of communication systems.

In terms of interference identification, researchers have used a variety of feature extraction and machine learning algorithms, such as the multi-parameter joint estimation method, fast independent component analysis and support vector machine, high-order cumulants and pattern recognition technology, to improve the recognition accuracy. With the development of deep learning, the application of deep learning algorithms based on convolutional neural networks, long short-term memory networks, etc. in interference identification is also gradually increasing.

2. Interference Types

2.1. Interference Patterns

The overall interference patterns include suppressive interference and deceptive interference. Suppressive interference can be further divided into barrage jamming and repeater jamming. This chapter mainly studies the impact of barrage jamming on Link 16.

(1) Comb-spectrum Barrage Jamming

The spectrum of comb-spectrum barrage jamming is comb-shaped, and the interference power is concentrated. However, it is necessary to obtain the frequency hopping communication band and frequency interval information, which is more complex. The spectrum distribution is shown in Figure 1.

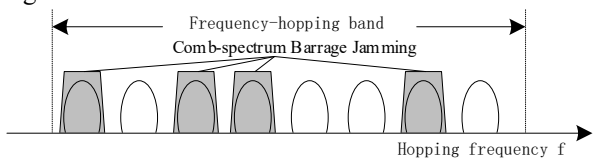

Figure 1. Schematic diagram of comb-spectrum barrage jamming

(2) Partial-band Barrage Jamming

Partial-band barrage jamming is a type of partial-band barrage jamming on the three frequency bands of the Link 16 signal. Its interference frequency domain effect is shown in Figure 2

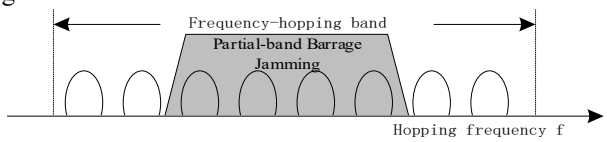

Figure 2. Schematic diagram of partial-band barrage jamming

(3) Wideband Barrage Jamming

Wideband barrage jamming covers the Link 16 channel. It

does not require frequency aiming, is easy to implement, and has a good interference effect. However, to cover multiple frequency points, a high power is required. The frequency domain effect diagram of wideband barrage jamming is shown in Figure 3

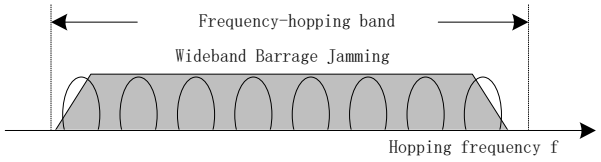

Figure 3. Schematic diagram of wideband barrage jamming

2.2. Interference Signals

This section studies several common interference signals.

(1) Single-tone Interference

The expression of single-tone interference is:

$$J(t) = Aexp\big(j(2\pi f_c t + \varphi)\big) \quad (1)$$

Where A is the amplitude, f_c is the interference frequency, and φ is the initial phase.

(2) Multi-tone Interference

Multi-tone interference is a complex baseband expression superimposed by multiple single-tone interferences:

$$J(t) = \sum_{m=1}^{m} A_m \, exp\big(j(2\pi f_m t + \varphi_m)\big) \quad (2)$$

Where A_m is the amplitude of the M single-tone interference of the multi-tone interference, and similarly,f_m and φ_m are the frequency and phase of the M single-tone interference, respectively.

(3) Partial-band Noise Interference

Partial-band interference is to concentrate the energy of the noise within the specified frequency band range, and its expression is:

$$J(t) = U(t) \, exp\big(j(2\pi f_c t + \varphi)\big) \quad (3)$$

Where *U(t)* obeys Gaussian noise with a mean of 0 and a variance of σ_n^2 ,f_c is the center frequency of the interference signal, and φ is the initial phase.

(4) Linear Sweep Frequency Interference

The frequency of linear sweep frequency interference has a linear relationship with time, and its time-domain expression is:

$$J(t) = Aexp\big(j(2\pi f_0 t + \varphi + \pi k t^2)\big) \quad 0 \le t \le T \quad (4)$$

Where $A$is the amplitude,f_0 is the initial frequency,φ is the initial phase, k is the frequency modulation coefficient, and T is the signal duration.

(5) Chirp Frequency Modulation Interference

The expression of a single-component Chirp signal is:

$$J(t) = Aexp\left(j2\pi\left(f_0 t + \frac{k_0}{2}t^2\right)\right) \quad 0 \le t \le T \quad (5)$$

Where A is the amplitude, f_0 is the initial frequency, k_0 is the frequency modulation slope of the signal, and T is the signal duration.

(6) Noise Frequency Modulation Interference

This interference is where the frequency has a linear relationship with the modulating Noise Voltage. Its expression is:

$$J(t) = Aexp\left(j\left(2\pi f_c t + k_{fm}\int_0^t \xi(t')\,\mathrm{d}t'\right)\right) \quad (6)$$

In the formula, A is the amplitude, f_c is the center frequency of the interference signal, k_{fm} is the frequency modulation coefficient, and $\xi(t)$ obeys Gaussian noise with a mean of 0 and a variance of σ_n^2 . The bandwidth of the interference signal is determined by the frequency modulation coefficient and the variance together.

(7) Noise Amplitude Modulation Interference

The expression of noise amplitude modulation interference is:

$$J(t) = (U_0 + U_n(t))cos\big(w_j t + \varphi\big) \quad (7)$$

Where U_0 is the carrier amplitude,w_j is the carrier angular frequency,$U_n(t)$ is the baseband noise, and φ is uniformly distributed within [0, 2π].

(8) Sawtooth Wave Frequency Modulation Interference

The sawtooth wave frequency modulation signal is frequency modulated using a sawtooth wave signal, similar to the noise frequency modulation signal. Its expression is:

$$J(t) = Acos(2\pi f_c t + 2\pi K\int m(t)\,dt) \quad (8)$$

Where A represents the amplitude, f_c is the carrier frequency of the signal, K is the modulation coefficient, and *m(t)* is the periodic sawtooth wave signal.

The following formula gives the power of the frequency component $f_c \pm nF$ in each frequency band of the sawtooth wave frequency modulation signal.

$$P_i = \frac{F}{4\Delta f_i}\left\{\left[C\left(\frac{\Delta f_i + nf}{\sqrt{\Delta f_i \cdot F}}\right) + C\left(\frac{\Delta f_i - nf}{\sqrt{\Delta f_i \cdot F}}\right)\right]^2 + \left[S\left(\frac{\Delta f_i + nf}{\sqrt{\Delta f_i \cdot F}}\right) + S\left(\frac{\Delta f_i - nf}{\sqrt{\Delta f_i \cdot F}}\right)\right]^2\right\} P_o \quad (9)$$

Where F is the periodic frequency of the sawtooth wave, $2\Delta f_i$ is the frequency deviation of the signal modulation, P_o is the total interference power, and C and S are Fresnel integrals.

When the frequency modulation bandwidth is very large, that is, $2\Delta f_i \gg F$,the F at this time can be ignored and can be simplified to the following formula:

$$P_i \approx \frac{F}{2\Delta f_i} P_o \quad (10)$$

From the above formula, it can be concluded that the sawtooth wave frequency modulation signal has $F/2\Delta f_i$ components, and the interference power of each component is basically the same, and is uniformly distributed in a comb-like manner in the available frequency band.

3. Interference Recognition Based on Deep Learning

Deep learning is an important branch in the field of machine learning. Its principle is mainly based on the concept of artificial neural networks, and realizes the learning and analysis of data by constructing a deep neural network model.

(1) Residual Network (CV-ResNet)

When the number of network layers continues to increase, problems of gradient dispersion or gradient explosion may occur, that is, when the neural network continues to deepen, then the network may show a degradation phenomenon. To solve this problem, He Kaiming's team proposed the Deep Residual Network (ResNet). Consider adding a new layer to the shallow layer of the network. The new layer is based on the identity transformation, that is, the input and output are an equal mapping relationship. In this case, the result obtained by the deep network should be the same as the result of the

shallow network, which greatly improves the network depth. The difference between the residual network and the convolutional neural network is that there is an additional residual block. The expression of the residual block is as follows:

$$X_{l+1} = X_l + F(X_l, W_l) \tag{11}$$

The framework of the residual block is shown in Fig 4.

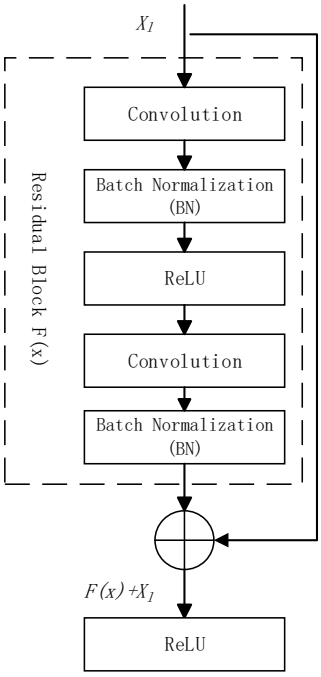

Figure 4. Residual Block Framework

F(x) is the key of the residual network. When the residual block is 0, the network performs an identity mapping.

4. Interference Recognition Network Based on CV-R-BiLSTM-A

(1) Data Preprocessing

The intensity of the interference signal may vary. In order to avoid the influence of different amplitudes, powers, etc. on the recognition performance, a power normalization operation is performed on the signal *x(n)*.

$$\bar{x}(n) = \frac{x(n)}{\sqrt{1/N \sum_{n=1}^{N} |x(n)|^2}} \tag{12}$$

Where *N* is the sampling point. When the original signal is collected using time-domain truncation, it will cause spectral energy loss, and using the Hanning window can reduce leakage.

(2) Network Input

The received signal sequence contains the interference signal and Gaussian noise. Its mathematical model is:

$$y = j + n \tag{13}$$

Where *j* is the interference signal and *n* is the Gaussian noise. The input data format is the *I* and *Q* paths of the interference signal. The network label selects the one-hot encoding of the signal category.

(3) Interference Recognition Structure Based on CV-R-BiLSTM-A

In the existing interference recognition methods, manual feature extraction is required, which has a high computational complexity and may result in incomplete or redundant feature extraction. In view of the shortcomings of the existing methods, this paper uses the deep learning method to identify the interference signal. An interference recognition network based on Complex valued Residual Bi Directional Long Short Term Memory Attention (CV-R-BiLSTM-A) is built, where CV represents complex convolution, R represents the residual network, and A represents the attention mechanism. The data of the interference signal generally includes two parts: the real part and the imaginary part. Most deep learning networks only study the real part of the signal, which will destroy the direct correlation between the real part and the imaginary part in the interference signal. Therefore, this paper will introduce the complex convolution network [70]. It is applied to the interference signal recognition. As the network depth increases, the network performance deteriorates. Therefore, when designing this network, a residual structure is proposed to address this problem, which can effectively solve the problem of gradient explosion. After extracting the features of the signal through convolution, the BiLSTM module is added to extract the temporal features of the interference signal using the BiLSTM module. Finally, the attention mechanism module is added to calculate the memory distribution of the features, distinguish the importance of the feature information, and use Softmax to classify the output to complete the recognition. The network structure diagram of CV-R-BiLSTM-A is shown in Fig 5.

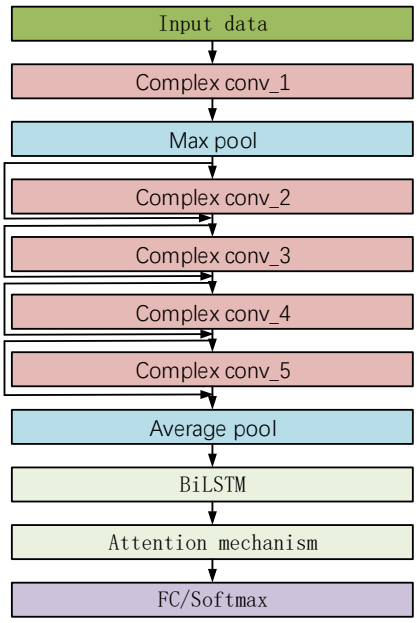

Figure 5. The structure diagram of the interference recognition network based on CV-R-BiLSTM-A

This network first inputs the processed data into the first convolutional layer for feature extraction, where the convolution kernel is 7 * 1 and the stride is 2; then the data passes through a maximum pooling layer with a stride of 2; then the data will pass through 4 convolutional layers Complex conv_2 ~ Complex conv_5, and a residual connection is constructed between the convolutional layers. The parameters of different convolutional layers are shown in Table 1.

The activation function selected is the CReLU function, and in order to improve the training speed of the network and effectively alleviate the problem of gradient loss, a BN layer is added before using the activation function in each convolutional layer. Then the data is input into BiLSTM, which is composed of two layers of LSTM with 256 neurons, and the activation function selected is sigmoid. The attention layer calculates the attention distribution in the feature

information, and then performs weighted summation on the input feature information. Finally, the result enters the fully connected layer and Softmax for the final classification.

Table 1. Model size of different convolutional layers.

Complex conv_x	Model size
Complex conv_1	7*1, 32, step length 2
Complex conv_2	(3*1, 32)*2
Complex conv_3	(3*1, 64)*2
Complex conv_4	(3*1, 128)*2
Complex conv_5	(3*1, 256)*2

5. Simulation Results and Analysis

(1) Parameter Settings

The simulation hardware environment uses GPU (NVIDIA RTX 3060), and the software uses Matlab and the deep learning framework TensorFlow. The network initialization method uses MSRA initialization, the loss function is cross-entropy, and the batch size is 16.

Eight types of interference signals are generated using Matlab. In the simulation, the sampling rate is set to 10 MHz, and Gaussian white noise is added to the channel. The dry noise ratio is defined as the ratio of the interference signal strength to the noise intensity within the communication frequency band. The dry noise ratio range is set to [-10:1:15] dB, and 2500 samples of each type of signal are randomly generated at each dry noise ratio. The number of samples in the training set, test set, and validation set is 6:2:2. After that, the experimental parameters remain the same as this.

(2) Analysis of the Effectiveness of the Network Model

Evaluation indicators:

Accuracy: The proportion of the total number of positive and negative samples correctly detected to the total number of samples.

$$Accuray = \frac{TN + TP}{TN + FP + TP + FN} \tag{14}$$

True Positive (TP), True Negative (TN), False Positive (FP), False Negative (FN). In this paper, when studying the recognition problem of eight types of interference signals, the accuracy rate is used to evaluate the recognition effect of the network model on the interference signals.

Precision: The probability that the actually positive samples in the predicted correct samples.

$$Precision = \frac{TP}{TP + FP} \tag{15}$$

Recall: The probability that the predicted positive samples in the actually positive samples.

$$Recall = \frac{TP}{TP + FN} \tag{16}$$

In order to verify the importance of each module of the designed network, three groups of ablation experiments were carried out. Training and testing were conducted under the same conditions. The overall recognition rate results of different networks for different interference signals in the test set within the dry noise ratio range of -10 dB to 15 dB are shown in Table 2.

Table 2. Ablation experiment based on CV-R-BiLSTM-A

Interference	CV-ResNet	CV-R-BiLSTM-A
Single-tone	80.2	90.2
Multi-tone	80.1	91.0
Linear Sweep Frequency	84.8	96.9
Noise Frequency Modulation	70.4	83.5
Noise Amplitude Modulation	74.4	84.0
Partial-band Noise	72.4	81.0
Chirp Frequency Modulation	74.1	86.9
Sawtooth Wave Frequency Modulation	80.7	92.3

It can be seen from the above table that the network with the highest recognition rate for the eight types of interference signals is the CV-R-BiLSTM-A network. Overall, using the CV-R-BiLSTM-A network has improved the overall recognition rate by about 10% compared to the CV-ResNet network.

(3) Simulation Effect Analysis and Comparison

After the CV-R-BiLSTM-A interference recognition network is trained, the test is carried out in the test set. The following Fig 6 is the confusion matrix of the CV-R-BiLSTM-A network under the dry noise ratio of -5 dB. The horizontal axis represents the label of the predicted value, and the vertical axis represents the label of the true value.

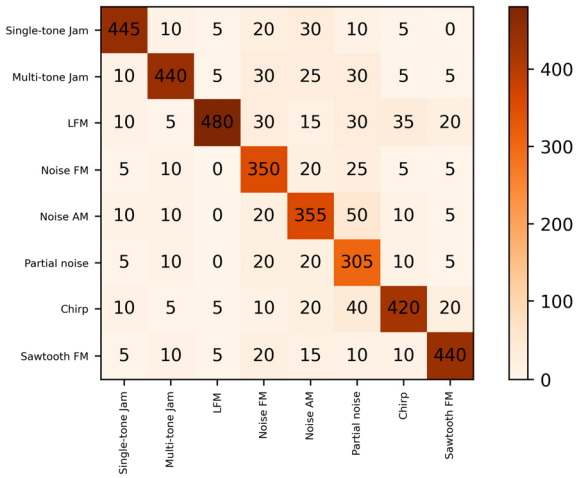

Figure 6. The confusion matrix of CV-R-BiLSTM-A network recognition under the dry noise ratio of -5 dB

Fig 7 is the confusion matrix of the CV-R-BiLSTM-A

network at 10 dB respectively.

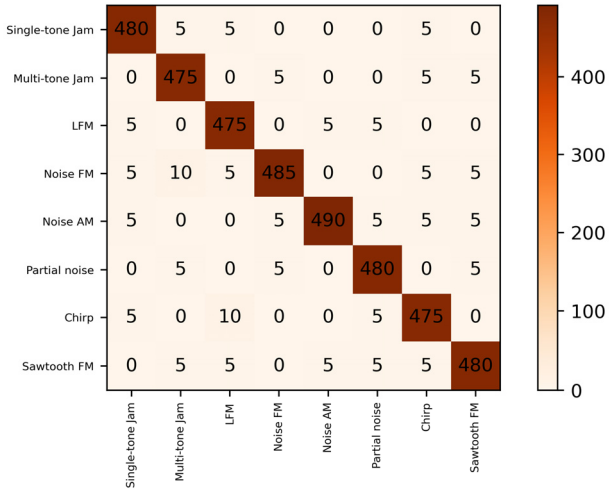

Figure 7. The confusion matrix of CV-R-BiLSTM-A network recognition under the dry noise ratio of 10 dB

It can be seen from the two confusion matrices that under a low dry noise ratio, the types with a poorer recognition effect using the CV-R-BiLSTM-A network are the three interference signals of noise frequency modulation, noise amplitude modulation, and partial noise, with a recognition rate of about 70%. Compared with the other several types of interference signals, the lowest recognition accuracy at this time can reach about 84%. Due to the fact that the characteristics of noise are not obvious under a low dry noise ratio, it can be seen from the confusion matrix that the three types of interference signals are misjudged evenly, and the misjudgments are not concentrated on a certain type of interference signal. However, compared with the case where the dry noise ratio is 10 dB, it can be found that as the interference increases, the network recognition accuracy has been improved, especially the recognition rates of the three signals of noise frequency modulation, noise amplitude modulation, and partial noise have all reached more than 95%.

The correct rate curve of the recognition rate of various interference signals under different dry noise ratios of the CV-R-BiLSTM-A network is shown in Fig 8.

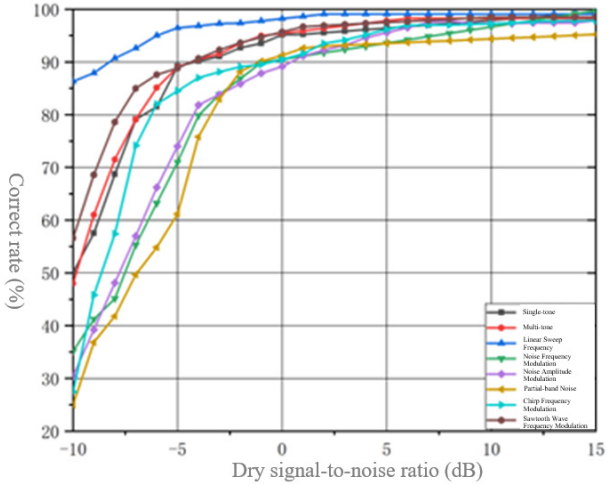

Figure 8. The interference recognition performance based on the CV-R-BiLSTM-A network

It can be seen from the graph that for each type of interference signal, the recognition accuracy increases with the increase of the dry noise ratio, and the network recognition accuracy tends to be stable after the dry noise ratio is greater than 8 dB. It can be intuitively seen from the graph that the recognition accuracy of the network for noise frequency modulation, noise amplitude modulation, and partial noise is relatively low when the dry noise ratio is less than 0 dB; the recognition effect of the network on linear sweep frequency interference is the best, and the accuracy can reach more than 90% at -5 dB.

In addition, the network designed in this chapter is compared with the existing networks in terms of network performance. The selected network models have been proven to be effective through a large number of experiments. Six networks are built for testing under the same simulation parameter design.

Table 3 gives the accuracy of several networks in recognizing interference signals.

Table 3. Comparison of interference recognition accuracy of different networks.

	CV-R-BiLSTM-A	LeNet-5	VGG16	ResNet34	Inception V4	AlexNet	DenseNet
Single-tone	90.31	85.42	84.52	87.48	89.48	86.48	88.28
Multi-tone	91.02	84.56	85.48	86.34	89.37	87.59	86.12
Linear Sweep Frequency	96.99	87.96	90.54	94.84	93.48	91.26	94.58
Noise Frequency Modulation	83.58	78.45	77.54	76.35	74.58	80.26	79.58
Noise Amplitude Modulation	84.08	81.54	80.45	81.35	80.91	79.81	76.58
Partial-band Noise	81.07	78.64	75.83	76.58	74.38	71.27	79.84
Chirp Frequency Modulation	86.97	81.34	82.45	83.48	82.57	85.18	79.84
Sawtooth Wave Frequency Modulation	92.33	84.56	90.48	82.46	91.48	86.48	89.48

It can be seen from the above table that the existing several networks only have better recognition effects on individual types of interference, for example, the AlexNet network has a better recognition effect on single-tone and multi-tone interference, the ResNet 34 and DenseNet networks have a better recognition effect on linear sweep frequency interference, and the VGG 16 network has a better recognition effect on sawtooth wave frequency modulation interference, but the recognition effects on noise frequency modulation, noise amplitude modulation, and partial noise are not outstanding. Overall, the CV-R-BiLSTM-A network has the best recognition effect on eight types of interference signals.

The curves of the overall recognition accuracy of different networks varying with the dry noise ratio are shown in Fig 9.

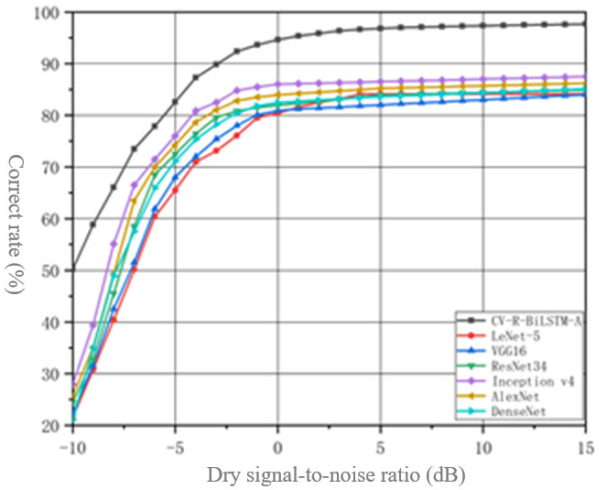

Figure 9. The performance comparison of different network models.

It can be seen from the figure that the CV-R-BiLSTM-A recognition network has a more obvious advantage in recognition effect compared to other networks. When the dry noise ratio is -5 dB, the network designed in this paper still has a recognition accuracy of approximately 50%, while other networks basically do not have the recognition ability at this time. After the dry noise ratio is greater than 5 dB, the CV-R-BiLSTM-A network has a more advantageous recognition ability, and the recognition rate can reach more than 95%, while the recognition rate of other networks is between 80% and 90% at this time. Through the presentation of the above figure and table, it is proved that the designed CV-R-BiLSTM-A network model is more suitable for the recognition and classification of these eight types of interference signals than the other several networks, reflecting the effectiveness of this network designed in this paper.

6. Conclusion

In response to the current problems of fewer interference signal recognition methods and the low overall recognition rate of interference recognition in existing methods, this paper proposes the CV-R-BiLSTM-A network to recognize interference signals. Adding a complex number module can extract signal features more completely, the BiLSTM module extracts temporal features, and the attention mechanism distinguishes the importance of features to improve the recognition accuracy. The results show that the overall recognition accuracy of the CV-R-BiLSTM-A network has been improved, but the network has a poor recognition rate for some noises, noise frequency modulation, and amplitude modulation at a low dry noise ratio.

References

[1] Mei Wenhua, CAI Shanfa. JTIDS/Link16 Data Link [M]. Beijing: National Defense Industry Press,2007.

[2] J-E Hwang, K Lee and S-H Jung. A Study on the Multi-Tactical Data Link Data Management [J]. The Journal of the Korea institute of electronic communication sciences, 2020, 15(3): 457 464.

[3] Lu Na. Data Link Theory and System [M]. 2nd edition. Beijing: Publishing House of Electronics Industry, 2018.

[4] C.Trabelsi, O.Bilaniuk, Y.Zhang, et al. Deep Complex Networks [J]. ArXiv, 2017, 1705.09792.

[5] K. He, X. Zhang, S. Ren, et al. Deep Residual Learning for Image Recognition[J]. ArXiv, 2016(6):770-778.

[6] Zhu Jialu, Ma Yongtao, Liu Kaihua. Multi-user joint anti-interference decision algorithm based on LSTM and DQN [J]. Chinese Journal of Sensor Technology, 2021, 34(06): 811-817. (in Chinese)

[7] Wei Yuning, Zhang Jindong, Li Yong et al. Automatic design method of Radar interference Signal Recognition Decision Tree [J]. Electro-optics and Control, 2019,27(04):82-86. (in Chinese)

[8] LI Wei. Research on interference technology of Link16 data link [D]. Xi 'an: Xidian University,2018.

[9] Zhao K, He F, Meng J, et al. Performance analysis of bit error rate of data Link system under pulse LFM interference in time-varying rayleigh channel[J]. Wireless Networks, 2021, 27(3): 1671-1681.

[10] Lee B, Jeong E, Choe S. Simulator for tactical data Link system with anti-jamming capability[C]. 2013 15th International Conference on Advanced Communications Technology (ICACT), PyeongChang, Korea (South), 2013: 789-793.

[11] Tan X, Yao C, Pan T, et al. Study on Link16 System with Frequency Hopping Collision Interference [J]. International Journal of Future Generation Communication and Networking, 2015, 8(2): 197-204.

[12] Ye F , Zhao T , Li Y , et al. Anti-interference Strategy Selection Method Based on the Minimum Loss Criterion[C]// 2020 IEEE USNC-CNC-URSI North American Radio Science Meeting (Joint with AP-S Symposium). IEEE, 2020.

[13] Sainath T N, Vinyals O, Senior A,et al. Convolutional, Long short-term memory, fully connected deep neural networks [C]. International Conference on Acoustics, Speech and Signal Processing. IEEE, 2015: 4580-4584.

[14] Mingfei Zhang, Zhoutao Yu, Zhenghua Xu. Short-term load forecasting usingrecurrent neural networks with input attention mechanism and hidden connection mechanism[J]. IEEE Access, 2020, 8: 186514-186529.